Cement Leakage in Percutaneous Vertebroplasty for Osteoporotic Compression Fractures With or Without Intravertebral Clefts

Noboru Tanigawa[1]
Shuji Kariya[1]
Atsushi Komemushi[2]
Takanori Tokuda[1]
Miyuki Nakatani[1]
Rie Yagi[1]
Satoshi Sawada[1]

OBJECTIVE. The purpose of our study was to compare the incidence and location of cement leakage in percutaneous vertebroplasty for osteoporotic compression fractures with and without intravertebral clefts.

MATERIALS AND METHODS. Percutaneous vertebroplasty was performed in 120 consecutive patients with 300 osteoporotic compression fractures. The cement volume injected was recorded. The cement leakage was evaluated using spinal radiography, MRI, and fluoroscopy during the procedure and CT after the procedure.

RESULTS. One hundred seven vertebrae contained intervertebral clefts, and 193 vertebrae had no clefts. The cement volume injected (± SD) was 4.0 ± 2.0 and 3.6 ± 1.6 mL into vertebrae with clefts and without clefts, respectively, with no statistically significant difference ($p = 0.14$). There was no statistically significant difference in the incidence of cement leakage between vertebrae with clefts (53 of 107) and those without clefts (78 of 193) ($p = 0.13$). Leakage occurred into the epidural veins (12 of 107), perivertebral soft tissues (7 of 107), disks (41 of 107), intervertebral foramen (1 of 107), and spinal canal (1 of 107) in fractures with clefts and into the epidural veins (47 of 193), perivertebral soft tissues (13 of 193), disks (25 of 193), paravertebral veins (5 of 193), large vein (2 of 193), lung (2 of 193), intervertebral foramen (1 of 193), and spinal canal (1 of 193) in fractures without clefts. Cement leakage into the epidural vein was significantly more frequent in vertebrae without clefts ($p < 0.01$). Disk leakage was significantly more frequent in vertebrae with clefts compared with those without clefts ($p < 0.01$).

CONCLUSION. There was no statistically significant difference in the incidence of cement leakage between vertebrae with clefts and without clefts. However, cement leakage into the epidural vein was significantly more frequent in vertebrae without clefts and disk leakage was significantly more frequent in vertebrae with clefts.

Keywords: cement leakage, clefts, osteoporosis, vertebroplasty

DOI:10.2214/AJR.09.2774

Received March 20, 2009; accepted after revision May 11, 2009.

[1]Department of Radiology, Kansai Medical University, Hirakata Hospital, 2-3-1 Shinmachi, Hirakata, Osaka, 573-1191, Japan. Address correspondence to N. Tanigawa (tanigano@hirakata.kmu.ac.jp).

[2]Department of Radiology, Kansai Medical University, Takii Hospital, Moriguchi, Osaka, Japan.

WEB
This is a Web exclusive article.

AJR 2009; 193:W442–W445

0361–803X/09/1935–W442

The intravertebral cleft is generally considered a radiographic sign of avascular necrosis of the vertebral body associated with impairment of the vertebral blood supply and cartilaginous nodes and normal stress placed on a weakened vertebra [1–3]. This sign is highly suggestive of osteonecrosis, although it is not specific [4] and has not been described in association with acute vertebral fractures [5]. In other words, clefts are thought to represent fracture nonunion [1, 2].

In percutaneous vertebroplasty, the existence of clefts inside fractured vertebral bodies is significant, and back pain disappears by injecting cement into clefts to relieve instability in the fractured vertebrae [6–12]. Reports have indicated that cement can be injected easily into clefts at low pressure with minimal cement leakage outside the vertebral body [13]. In addition, kyphoplasty is a technique that prepares a gap, or cleft, in a fractured vertebral body using a balloon and then cement is injected. Compared with vertebroplasty, the degree of cement leakage outside the vertebra is lower for kyphoplasty [14, 15]. However, while the cement is being injected into a cleft during percutaneous vertebroplasty, cement sometimes leaks into the intervertebral disk connected to the cleft.

Leakage into the intervertebral disk is often asymptomatic but has been reported as one cause of new compression fractures after percutaneous vertebroplasty [14, 16, 17], and therefore leakage must be minimized. The purpose of this study was to compare the incidence and location of cement leakage in percutaneous vertebroplasty for osteoporotic compression fractures with and without intravertebral clefts.

Materials and Methods

This study was conducted on 120 consecutive patients (107 women, 13 men) with painful osteoporotic compression fractures treated using percutaneous vertebroplasty. The mean patient age was 73 years (age range, 44–86 years). A total of 300 vertebral bodies were treated. Locations and numbers of treated vertebral bodies were as follows: T5, $n = 2$; T6, $n = 5$; T7, $n = 7$; T8, $n = 13$; T9, $n = 11$; T10, $n = 11$; T11, $n = 23$; T12, $n = 50$; L1, $n = 63$; L2, $n = 34$; L3, $n = 43$; L4, $n = 23$; and L5, $n = 15$.

The indication for percutaneous vertebroplasty was back pain caused by vertebral body compression fracture, with pain on percussion of the vertebral spinous process. In cases with multiple compression fractures in which percussion pain of the spinous process was unclear, physical examination was performed using fluoroscopy. Patients with back pain attributed to myelopathy or radiculopathy resulting from stenosis of the vertebral canal or narrowing of the intervertebral foramen were excluded.

Percutaneous Vertebroplasty Procedure

Informed consent was obtained from all patients before the procedure. All procedures were performed by one of the authors who had 9 years of experience in percutaneous vertebroplasty or by a fellowship trainee under the supervision of the author. Percutaneous vertebroplasty was performed under combined CT and fluoroscopic guidance (Advantx LCA plus ACT, GE Healthcare). Thirty minutes preoperatively, 10 mg of morphine hydrochloride, 0.5 mg atropine sulfate, and 25 mg hydroxyzine hydrochloride were administered intramuscularly. Local anesthesia with 10 mL of 1% lidocaine was administered from the skin to the periosteum of the pedicle using a 22-gauge Cathelin needle (Terumo Europe) under fluoroscopic guidance. After orientation of the puncture needle was confirmed on CT and aligned with the Cathelin needle, a 13-gauge bone biopsy needle (Osteo-Site Bone Biopsy Needle Murphy M2, Cook) was advanced into the pedicle of the vertebral arch. A unilateral transpedicular approach was chosen in all cases. CT was repeated, and after the orientation of the biopsy needle was confirmed, the visualization technique was changed to lateral fluoroscopy and the bone biopsy needle was advanced to the anterior third of the vertebral body close to the midline.

Intraosseous venography was performed with 1–5 mL of iopamidol (Iopamiron 300, Schering Japan) or 5–20 mL of carbon dioxide to confirm that the needle was not positioned within a direct venous anastomosis to the central or epidural veins. Subsequently, 20 g of methylmethacrylate powder (Osteobond Copolymer Bone Cement, Zimmer) was mixed with 5 g of barium sulfate powder that had been sterilized with dry heat to increase its opacity. Next, 10 mL of liquid methylmethacrylate monomer was added to the powder, and the mixture was blended to a toothpastelike consistency, producing polymethylmethacrylate (PMMA). Using 1-mL syringes, the PMMA was injected with lateral fluoroscopic guidance. PMMA injection was terminated when adequate filling of the vertebral body was achieved or if leakage occurred. When a fractured cleft was filled with cement for the cases with clefts, we stopped the cement injection. The needle was then removed, and all patients were observed in the supine position for 2 hours.

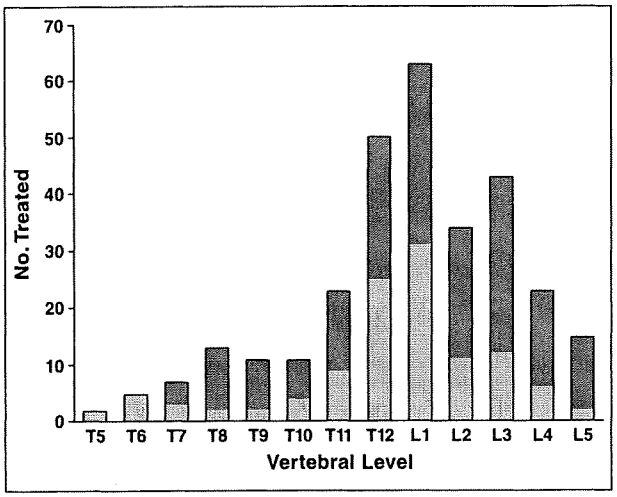

Fig. 1—Graph shows distribution of treated vertebral fractures. Light gray shading indicates without intravertebral clefts and dark gray shading indicates with intravertebral clefts.

Cleft and Leakage Diagnosis

Clefts were diagnosed on the basis of linear well-demarcated radiolucency inside a fractured vertebral body on preoperative radiography or, alternatively, using transverse signal hyperintensities on fat-suppressed T2-weighted MRI. Furthermore, linear well-demarcated radiolucency seen by intraoperative fluoroscopy and lesions in which cement was injected as compact and solid cement filling during PMMA injection were diagnosed as clefts. In addition, CT was performed immediately after PMMA injection, and compact and solid cement fillings also were diagnosed as clefts. Leakage outside vertebral bodies was assessed by CT immediately after PMMA injection, and 3D images were prepared to diagnose leakage location. Images including spinal radiography, MRI, and CT were evaluated by two of the authors who reached a consensus for each case. Chest radiographs were obtained to detect pulmonary cement embolism 1 day after percutaneous vertebroplasty. When a pulmonary cement embolism was suspected during the procedure, chest CT was performed immediately after the procedure.

Statistical Analysis

The volume of cement injection per vertebra was compared between vertebral bodies with and without clefts and analyzed using the Wilcoxon's rank-sum test. The chi-square test was used to compare occurrence rates of cement leakage.

TABLE 1: Cement Leakage Outside Vertebra With or Without Cleft

Location	With Cleft ($n = 107$)	Without Cleft ($n = 193$)	p
Epidural vein	12 (11.2)	47 (24.4)	> 0.01
Perivertebral soft tissue	7 (6.5)	13 (6.7)	0.95
Intervertebral disk	41 (38.3)	25 (13.0)	> 0.01
Paravertebral vein	0 (0)	5 (2.6)	0.09
Large vein[a]	0 (0)	2 (1.0)	0.29
Lung	0 (0)	2 (1.0)	0.29
Intervertebral foramen	1 (0.9)	1 (0.5)	0.67
Spinal canal	1 (0.9)	1 (0.5)	0.67
Total	62 (57.9)	96 (49.7)	

Note—Data are number of patients, and numbers in parentheses are percentages.
[a]Mean inferior vena cava and azygos vein.

All statistical analyses were conducted using StatView for Windows version 5.0 software (SAS Institute), and values of $p < 0.05$ were considered statistically significant.

Results

One hundred seven vertebrae contained intervertebral clefts, and 193 vertebrae had no clefts. Forty-three (40.2%) and 71 (66.4%) of 107 clefts were detected on spine radiography and MRI, respectively. On the other hand, 36 of 107 clefts (33.6%) were diagnosed on fluoroscopy during the procedure or on CT after the procedure. Locations of each vertebra are shown in Figure 1.

The mean volume of cement injected (± SD) was 4.0 ± 2.0 mL for vertebrae with clefts and 3.6 ± 1.6 mL for vertebrae without clefts, and the volumes were not significantly different ($p = 0.14$). There was no statistically significant difference in the incidence of cement leakage between vertebrae with clefts (53 of 107 vertebrae, 49.5%) and those without clefts (78 of 193 vertebrae, 40.4%) ($p = 0.13$). Leakage locations included the epidural vein (12 of 107, 11.2%), perivertebral soft tissue (7 of 107, 6.5%), intervertebral disk (41 of 107, 38.3%) (Fig. 2), intervertebral foramen (1 of 107, 0.9%), and spinal canal (1 of 107, 0.9%) in fractures with clefts; and the epidural vein (47 of 193, 24.4%) (Fig. 3), perivertebral soft tissues (13 of 193, 6.7%), intervertebral disk (25 of 193, 13.0%), paravertebral vein (5 of 193, 2.6%), large veins including the inferior vena cava and azygos vein (2 of 193, 1%), lung (2 of 193, 1%), intervertebral foramen (1 of 193, 0.5%), and spinal canal (1 of 193, 0.5%) in fractures without clefts (Table 1). Cement leakage into the epidural vein was significantly more frequent in vertebrae without clefts compared with those with clefts ($p < 0.01$). On the other hand, disk leakage was significantly more frequent in vertebrae with clefts than in those without clefts ($p < 0.01$) (Table 1).

Symptomatic cement leakage developed in only four patients. One patient had radiculopathy caused by a large cement leak into the adjacent disk. Continuous pain for about 1 month at the puncture site caused by cement leakage into subcutaneous tissue through the needle track developed in three patients. No patients had symptoms from the epidural leakage.

Discussion

The presence or absence of clefts was diagnosed using not only preoperative radiography and MRI but also intraoperative fluoroscopy and the distribution of PMMA after injection on CT. The reason for these varying methods of detection was that the detection rate of clefts is low using preoperative diagnostic imaging alone, and in some cases clefts can be seen only after injecting PMMA [6, 17–19].

The amount of injected PMMA was greater for vertebral bodies with clefts compared with vertebral bodies without clefts, although there was no statistically significant difference in the volume of PMMA injected. In vacuum clefts containing gas or fluid, the level of resistance during cement injection was low because of low pressure inside the clefts, allowing a greater amount of cement into the cleft and increasing the cleft volume [5, 20].

There was no statistically significant difference in the incidence of cement leakage between vertebrae with clefts and those without clefts. These results agree with the report by Jung et al. [21], but Krauss et al. [15] reported that the incidence of leakage was lower for vertebral bodies with clefts than those without clefts. Krauss et al. indicated that cement leakage occurred in 18.2% (8 of 44) of clefts, whereas cement leakage occurred in 49.5% (53 of 107) of clefts in our series. The leakage rate of our series was significantly higher than in the series of Krauss et al. The mean cement volume injected by Krauss et al. was 3.1 mL, and the mean was 4.0 mL in our series. The cement volume injected was greater in our series than in that of Krauss et al. However, because Krauss et al. did not describe the end point of cement injection, the difference between their study and ours is not clear. Ha et al. [22] likewise reported that the incidence of leakage was higher for vertebral bodies with clefts compared with those without clefts.

Fig. 2—79-year-old woman with vertebral compression fracture with cleft of T12 due to osteoporosis. Sagittal CT image shows cement leakage into disk through part of destroyed endplate.

The incidence of leakage into the intervertebral disk was significantly higher for vertebral bodies with clefts than for vertebral bodies without clefts. The current study and the investigation by Jung et al. [21] were the only ones that have addressed the location of cement leakage from vertebral bodies with clefts, and our results agreed with the results obtained by Jung et al. The reason for cement leakage from vertebral bodies with clefts is

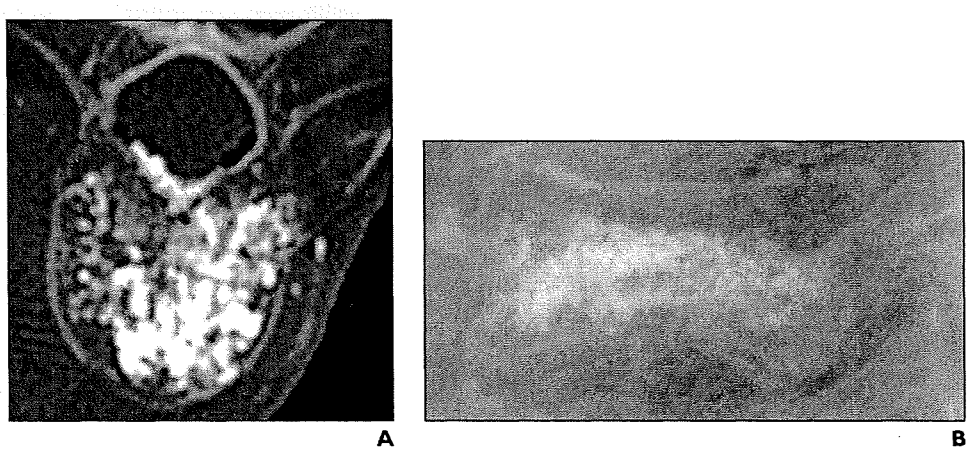

Fig. 3—73-year-old woman with vertebral compression fracture without cleft of T7 due to osteoporosis.
A, CT scan shows bone cement in epidural vein continuing to vertebral body. Cleft is not detected in fractured vertebral body.
B, Lateral spinal radiograph shows opaque cement interspersed through trabecular space.

primarily endplate damage, which is high for vertebral bodies with clefts, allowing cement to leak into the intervertebral disk via endplate damage. Furthermore, studies have reported that the vacuum phenomenon in vertebral bodies is associated with the vacuum phenomenon in the intervertebral disk [6, 23].

For vertebral bodies without clefts, leakage into the perivertebral veins occurred most commonly. The cancellous bone of vertebral bodies contains a rich internal vasculature that communicates with the epidural plexus and segmental veins. Moreover, we applied unilateral injection of cement in all cases. At the unilateral injection, the needle-tip is positioned on the midline of the vertebra. Basivertebral veins are primarily distributed in the midline portion of the vertebra. We think that a part of the cement was injected into the basivertebral veins and then leaked into the epidural veins. Therefore, cement injected into vertebral bodies readily leaks into veins through these passages [24].

Some limitations exist in the current study. First, the study was retrospective and only examined a small number of vertebral bodies. Second, all procedures were not performed by only one operator.

Injecting cement into clefts is easy, and fluoroscopy during injection shows that the height of vertebral bodies increases during injection. This tempts operators to inject more cement. However, our findings show that the incidence of cement leakage into the intervertebral disk is significantly higher in vertebral bodies with clefts, and leakage into the intervertebral disk may induce new compression fractures [11, 13, 14]. Caution must therefore be exercised during cement injection while keeping these points in mind.

In conclusion, there was no statistically significant difference in the incidence of cement leakage between vertebrae with clefts and those without clefts. However, cement leakage into the epidural vein was significantly more frequent in vertebrae without clefts compared with those with clefts, and leakage into the intervertebral disk was significantly more frequent in vertebrae with clefts than in those without clefts.

References

1. Kumpan W, Salomonowitz E, Seidl G, Wittich GR. The intravertebral vacuum phenomenon. *Skeletal Radiol* 1986; 15:444–447
2. Shih TT, Tsuang YH, Huang KM, Chen PQ, Su CT. Magnetic resonance imaging of vertebral compression fractures. *J Formos Med Assoc* 1996; 95:313–319
3. Benedek TG, Nicholas JJ. Delayed traumatic vertebral body compression fracture. Part II. Pathologic fractures. *Semin Arthritis Rheum* 1981; 10: 271–277
4. Resnick D. Vertebral body. In: Resnick D, ed. *Diagnosis of bone and joint disorders*, 3rd ed. Philadelphia, PA: Saunders, 1995:3527–3530
5. Maldague BE, Noel HM, Malghem JJ. The intravertebral vacuum cleft: a sign of ischemic vertebral collapse. *Radiology* 1978; 129:23–29
6. Lane JI, Maus TP, Wald JT, Thielen KR, Bobra S, Luetmer PH. Intravertebral clefts opacified during vertebroplasty: pathogenesis, technical implications, and prognostic significance. *AJNR* 2002; 23:1642–1646
7. Mirovsky Y, Anekstein Y, Shalmon E, Peer A. Vacuum clefts of the vertebral bodies. *AJNR* 2005; 26:1634–1640
8. Carlier RY, Gordji H, Mompoint DM, Vernhet N, Feydy A, Vallée C. Osteoporotic vertebral collapse: percutaneous vertebroplasty and local kyphosis correction. *Radiology* 2004; 233:891–898
9. Kim DY, Lee SH, Jang JS, Chung SK, Lee HY. Intravertebral vacuum phenomenon in osteoporotic compression fracture: report of 67 cases with quantitative evaluation of intravertebral instability. *J Neurosurg* 2004; 100[1 suppl spine]:24–31
10. Peh WC, Gelbart MS, Gilula LA, Peck DD. Percutaneous vertebroplasty: treatment of painful vertebral compression fracture with intraosseous vacuum phenomena. *AJR* 2003; 180:1411–1417
11. McKiernan F, Faciszewski T. Intravertebral clefts in osteoporotic vertebral compression fractures. *Arthritis Rheum* 2003; 48:1414–1419
12. Mathis JM. Vertebroplasty for vertebral fractures with intravertebral clefts. *AJNR* 2002; 23:1619–1620
13. Lin EP, Ekholm S, Hiwatashi A, Westesson PL. Vertebroplasty: cement leakage into the disc increases the risk of new fracture of adjacent vertebral body. *AJNR* 2004; 25:175–180
14. Komemushi A, Tanigawa N, Kariya S, et al. Percutaneous vertebroplasty for osteoporotic compression fracture: multivariate study of predictors of new vertebral body fracture. *Cardiovasc Intervent Radiol* 2006; 29:580–585
15. Krauss M, Hirschfelder H, Tomandl B, Lichti G, Bär I. Kyphosis reduction and the rate of cement leaks after vertebroplasty of intravertebral clefts. *Eur Radiol* 2006; 16:1015–1021
16. Theodorou DJ, Theodorou SJ, Duncan TD, Garfin SR, Wong WH. Percutaneous balloon kyphoplasty for the correction of spinal deformity in painful vertebral body compression fractures. *Clin Imaging* 2002; 26:1–5
17. Garfin SR, Reilley MA. Minimally invasive treatment of osteoporotic vertebral body compression fractures. *Spine J* 2002; 2:76–80
18. Trout AT, Kallmes DF, Lane JI, Layton KF, Marx WF. Subsequent vertebral fractures after vertebroplasty: association with intraosseous clefts. *AJNR* 2006; 27:1586–1591
19. Wiggins MC, Sehizadeh M, Pilgram TK, Gilula LA. Importance of intravertebral fracture clefts in vertebroplasty outcome. *AJR* 2007; 188:634–640
20. Golimbu C, Firooznia H, Rafii M. The intravertebral vacuum sign. *Spine* 1986; 11:1040–1043
21. Jung JY, Lee MH, Ahn JM. Leakage of polymethylmethacrylate in percutaneous vertebroplasty: comparison of osteoporotic vertebral compression fractures with and without an intravertebral vacuum cleft. *J Comput Assist Tomogr* 2006; 30:501–506
22. Ha KY, Lee JS, Kim KW, Chon JS. Percutaneous vertebroplasty for vertebral compression fractures with and without intravertebral clefts. *J Bone Joint Surg Br* 2006; 88:629–633
23. Lafforgue P, Chagnaud C, Daumen-Legre V, Daver L, Kasbarian M, Acquaviva PC. Intravertebral vacuum phenomenon ("vertebral osteonecrosis"): migration of intradiscal gas in a fractured vertebral body. *Spine* 1997; 22:1885–1891
24. Groen RJM, du Toit DF, Phillips FM, et al. Anatomical and pathological considerations in percutaneous vertebroplasty and kyphoplasty. *Spine* 2004; 29:1465–1471

ORIGINAL ARTICLE

ACTA RADIOLOGICA

Composite Material Stent Comprising Metallic Wire and Polylactic Acid Fibers, and its Mechanical Strength and Retrievability

Y. SHOMURA, N. TANIGAWA, T. TOKUDA, S. KARIYA, H. KOJIMA, A. KOMEMUSHI & S. SAWADA
Department of Radiology, Kansai Medical University, Hirakata Hospital, Osaka, Japan

Shomura Y, Tanigawa N, Tokuda T, Kariya S, Kojima H, Komemushi A, Sawada S. Composite material stent comprising metallic wire and polylactic acid fibers, and its mechanical strength and retrievability. Acta Radiol 2009;50:355–359.

Background: Although metallic stents are characterized by strong expanse of force, thin walls, and easy stent deployment, their removal from the body is usually difficult or impossible due to the difficulty of unraveling their mesh structure. A stent built of a composite material comprising a metallic wire and a polylactic acid (PLA) fiber, in which the metallic wire component could be unraveled after PLA fiber degradation in the body, should allow easy stent removal.
Purpose: To evaluate the mechanical strength and retrievability of a composite material stent comprising a metallic wire and a PLA fiber.
Material and Methods: We produced a composite material stent comprising a metallic wire and a biodegradable fiber (hybrid stent). As the metallic wire is not cross-linked with itself, but with the PLA fibers only, the hybrid stent can be easily unraveled after PLA fiber degradation. This stent was built with a 0.2-mm stainless-steel wire and a 0.23-mm PLA fiber knitted in the same textile as an Ultraflex stent. For comparison, an identical stent was built using PLA fiber only (PLA stent). The mechanical strength of these stents was tested by the radial expansive force response against circumferential shrinkage stress load. Change in radial force due to PLA fiber degradation was estimated by adding an artificial PLA degeneration process, by immersing each stent in a water bath at 80°C for 48 hours. Retrievability of the hybrid stent after PLA degeneration was examined by hooking and pulling out the residual stainless-steel wire from a silicon tube.
Results: The hybrid stent exhibited a linear response in radial expansive force within the range of 15% diameter reduction. The PLA stent did not exhibit linear response at over 15% diameter reduction. Decrease of radial expansive force after PLA degradation was within 5% of the original force in the hybrid stent, but the PLA stent did not create effective radial expansive force. Hybrid stents, even after PLA degradation, exhibited a linear response in radial expansive force, within the range of 15% diameter reduction. The metallic component of the heat-processed hybrid stent was easily unraveled by pulling out the wire.
Conclusion: The hybrid stent comprising a stainless-steel wire and a PLA fiber appears to provide effective radial expansive force and retrievability.

Key words: Experimental investigation; interventional; retrievable; stents; thorax; tracheobronchial tree

Yuzo Shomura, Department of Radiology, Kansai Medical University, Hirakata Hospital, 2-3-1 Shinmachi, Hirakata, Osaka 573-1191, Japan (tel. +81 72 804 0101, fax. *+81 72 804 2865, e-mail. shomura@hirakata.kmu.ac.jp)*

Accepted for publication January 2, 2009

Metallic stents are characterized by a strong expanse of force, thin walls, and easy deployment not requiring general anesthesia. They are widely applied, not only for permanent but also for temporary stenting purposes, including strictures of benign etiology (1, 2) or diseases in children (3, 4). Once placed in the body, however, removal of a metallic stent is usually difficult or impossible (5–7). Occasionally, however, removal or replacement of a metallic stent is necessary, such as in cases with stent fracture or restenosis caused by cell proliferation. This may be accomplished by cutting the stent

informa
healthcare

DOI 10.1080/02841850902774600

wire loops to unravel the mesh structure or by the withdrawal of the structure as a whole by force. However, this may lead to severe complications, such as vessel and/or ductal rupture, causing bleeding that may result in further treatment difficulties.

SONG et al. reported on a metallic stent with a retrieval hook, which allows easy stent removal by pulling the hook after attachment to the stent body (8). The retrieval hook is useful for certain types of metallic stent structures, but may not be applied to all types of stent textile patterns, as some cannot be folded up sufficiently by merely pulling the stent outward.

In the present study, we built a composite material stent comprising a metallic wire and a polylactic acid (PLA) fiber (hybrid stent), in which the metallic wire component was not cross-linked with itself, but only with the PLA fiber. The metallic component therefore could easily be unraveled and straightened by pulling after the PLA fiber had degraded, allowing easy stent removal. The purpose of this study was to evaluate the mechanical strength of the hybrid stent and to examine its retrievability after PLA fiber degradation.

Material and Methods

Stent structure

An American National Standard of Industry (ANSI) 304-grade stainless-steel wire of 0.2 mm in diameter and a 0.23-mm PLA monofilament fiber (520T; Chukoh Chemical Industries, Ltd., Fukuoka, Japan) were cross-knitted in the same textile pattern as a commercial Ultraflex stent (Boston Scientific Co., Natick, Mass., USA) (Fig. 1). The stent size was 20 mm in diameter and 60 mm in length.

For comparison of mechanical strength, an identical test stent of the PLA monofilament fiber only (PLA stent), an Ultraflex stent, and a Spiral Z stent (Medicos Hirata Co., Tokyo, Japan) were prepared.

Evaluation of mechanical strength

Mechanical strength of the test stents was evaluated as the radial expansive force response against circumferential shrinkage stress load, as described previously (9). In summary, a test stent covered with a non-stretchable film was placed on a board fixed to one end of the covering film. The other end of the film was connected to a push/pull gauge (Imada Co., Toyohashi, Japan). Shrinkage load was added to the stent by pulling the film. The load added to the stent for stent diameter change was recorded four times, and the mean value was defined as the radial expansive force (Fig. 2).

Radial expansive force of a highly compressed stent was evaluated by adding a surface load (horizontal compression load) diametrically to the stent using a universal testing machine (RTC-1350A; Orientec Co., Tokyo, Japan). A test stent was attached between two metallic plates installed to the testing machine, and the upper metallic plate was lowered until the stent diameter was 10 mm (50% of its original diameter). Load value at this point was recorded by means of an autograph connected to the upper plate, and defined as radial expansive force at 50% diameter reduction (Fig. 3). Measurement was performed four times, and the

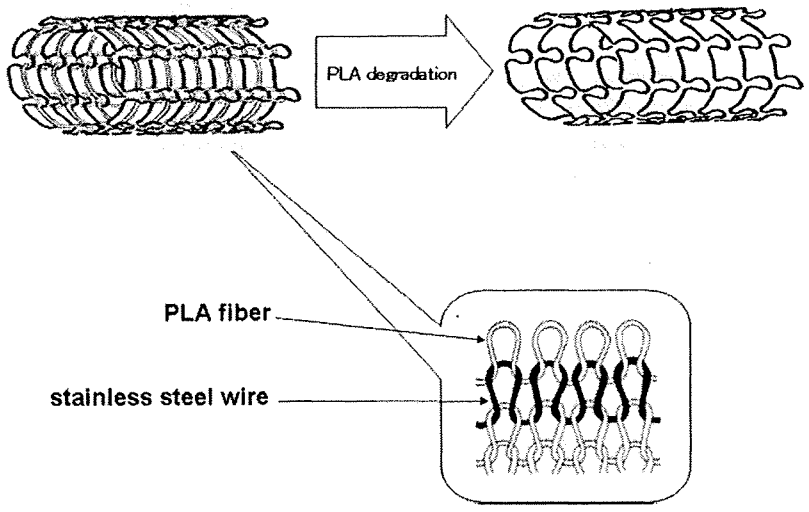

Fig. 1. Schematic structure of the hybrid stent. A stainless-steel wire and a PLA monofilament fiber were knitted in the same textile structure as the Ultraflex stent. The non-cross-linked metallic wire can be straightened after PLA fiber degradation, and easily removed.

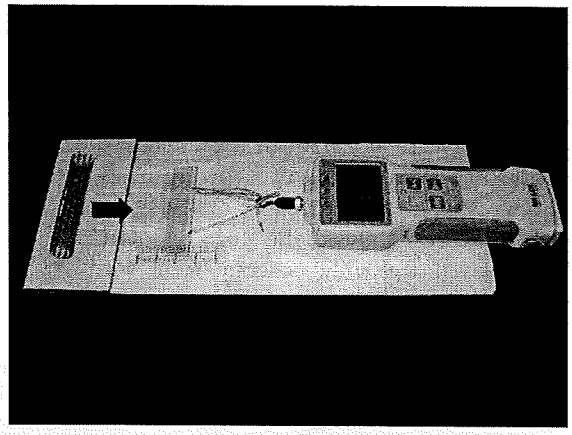

Fig. 2. Radial expansive force was evaluated as the resilient force response against circumferential shrinkage stress load applied to the test stent.

mean value was defined as the mean radial expansive force. Destruction and/or deformity of the stent, if any, were also recorded.

To estimate change of radial expansive force after PLA fiber degradation, an artificial PLA degradation process was added to the test stents (hybrid stent and PLA stent) by immersing them in a water bath at 80°C for 48 hours. The change in radial expansive force was compared to the original values.

Retrievability of metallic-core component

The hybrid stent with a 20-mm outer diameter, which underwent the heating process mentioned above, was set in a silicone tube of 18 mm inner diameter, i.e., the stent was set with 11% over-sizing relative to the diameter of the silicone tube. One end of the metallic-core component was grasped using forceps and pulled outward to unlock the spiral structure. Torsion of the metallic wire, stent displacement, resistance in the unlocking process, and deformities in the core were visually evaluated.

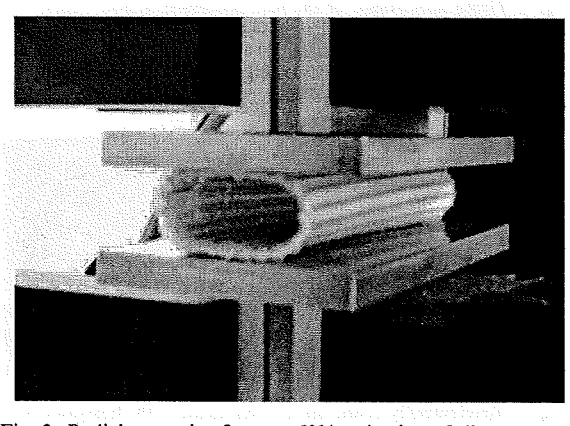

Fig. 3. Radial expansive force at 50% reduction of diameter was evaluated by adding a horizontal compression load diametrically to the stent using a universal testing machine. Destruction and/or deformity of the stent, if any, were also recorded.

Statistical analysis

The Wilcoxon rank-sum test was used to compare radial expansive force between the non-heated hybrid stent and the PLA stent. A P value of less than 0.05 was considered to indicate a statistically significant difference. All analyses were performed using StatView software (version 5.0; SAS Institute, Cary, N.C., USA).

Results

Mechanical strength

The hybrid stent exhibited linear radial expansive force response up to a point within the range of 15% diameter reduction. For the PLA stent, the lumen was obstructed at 15% diameter reduction, and did not exhibit radial expansive force increase over this point (Fig. 4). At 15% diameter reduction, radial expansive force was 33.0 N for the hybrid stent, 18.9 N for the PLA stent, 16.0 N for the Ultraflex stent, and 2.4 N for the Spiral Z stent. Radial expansive force of the hybrid stent was significantly higher than that of the other stents ($P=0.02$).

At 50% diameter reduction, the radial expansive force was 86.8 N for the hybrid stent, 21.1 N for the PLA stent, 36.8 N for the Ultraflex stent, and 20.8 N for the Spiral Z stent (Table 1). The radial expansive force of the hybrid stent at 50% diameter reduction was also significantly higher than that of other stents ($P=0.02$). However, the hybrid stent exhibited partial stent deformity after releasing the compression load (Fig. 5).

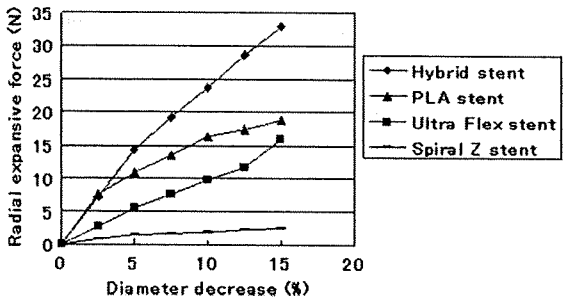

Fig. 4. Radial expansive force response against circumferential shrinkage stress load. The hybrid stent presented linear radial expansive force increase within the range of 15% reduction of the original diameter. In the PLA stent, linear response was lost when the diameter decreased by 15%.

Table 1. Radial expansive force at 50% reduction of diameter

Type of stent	Radial expansive force, N
Hybrid	86.8
PLA	21.1
Ultraflex	36.8
Spiral Z	20.8

The hybrid stent undergoing the heat process showed a slight decrease in radial expansive force, but it was not more than 5% of the original value within the range of a 15% diameter reduction. In contrast, the PLA stent did not exhibit effective radial expansive force, and was destroyed at 12% diameter reduction (Fig. 6). The hybrid stent maintained its original shape even after PLA degradation. In contrast, the PLA stent was easily crushed by adding slight compression loads (Fig. 7).

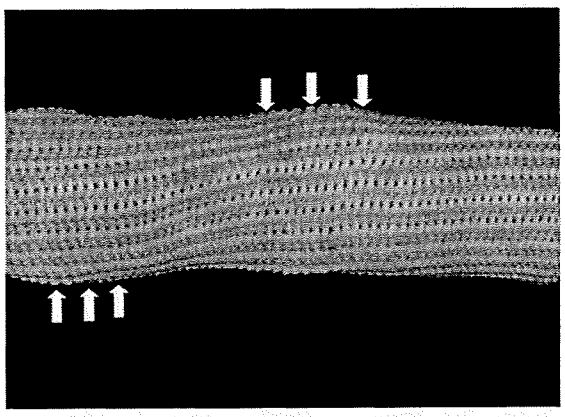

Fig. 5. Gross appearance of the hybrid stent after 50% diameter reduction. After being released from the compression load, slight deformity on the outer surface was observed (arrow).

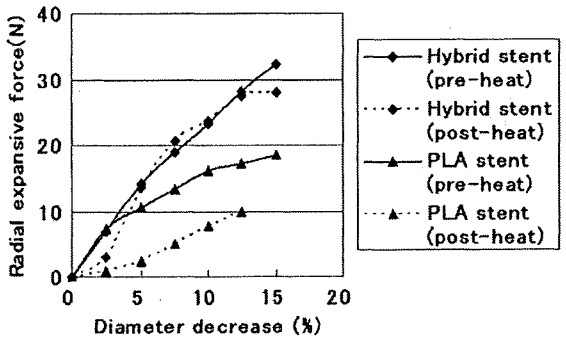

Fig. 6. Radial expansive force response of the heat-processed stents. The radial expansive force decrease of the hybrid stent was within 5% of the original force. The PLA stent did not exhibit effective radial expansive force after the heating process.

Retrievability of metallic-core component

After the heat process, the non-cross-linked metallic core of the hybrid stent was easily straightened by pulling the end of the stent wire. There was a slight displacement of the stent in the silicone tube while pulling the wire, but no excessive resistance, deformity, or torsion of the core was observed. As a result, the residual metallic-core component could be removed from the silicone tube without any difficulties (Fig. 8).

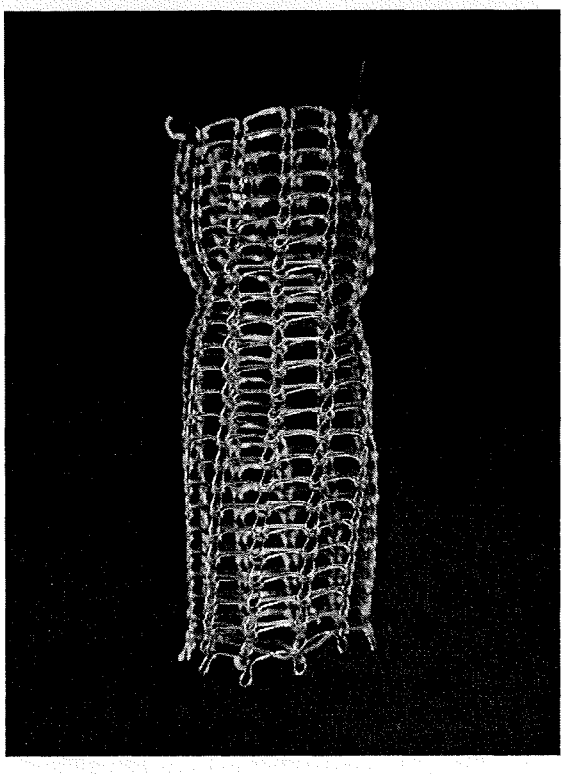

Fig. 7. Gross appearance of the heat-processed hybrid stents. The hybrid stent maintained its original shape, even after PLA degradation, but the PLA stent was destroyed with slight compression.

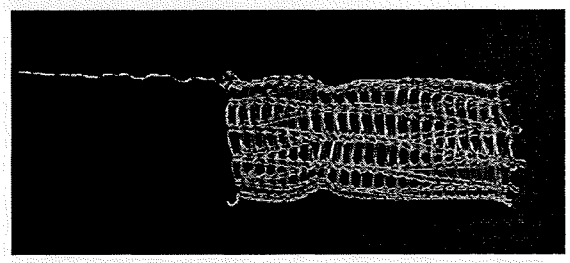

Fig. 8. Retrievability of the metal component of the heat-processed hybrid stent. The non-cross-linked metal core was easily straightened by pulling the end of the stent wire, and was removed from a silicone tube without difficulty.

Discussion

A combination of materials with different mechanical strengths has been used in the design of dynamic stents (10), in which a silicone plate and elastic rubber were successfully combined to achieve excellent conformability with tracheal wall movement. Our composite material stent is another attempt to use different materials in order to improve the retrievability of metallic knitted stents.

It seems that the mechanical strength of the hybrid stent is dependent on the metallic spiral component, because apparent reduction of the radial expansive force was not observed between before and after the artificial PLA degradation process. In addition, radial expansive force of the hybrid stent was higher than that of commercial stents such as the Ultraflex stent or the Spiral Z stent. This result was probably due to the use of a stiff wire used as the metallic spiral component. Furthermore, the radial expansive force of the hybrid stent may not only be due to the material factors of the metallic wire, but also structural factors of the metallic component, such as circumferential loop density and/or length of the loop leg.

Our study was limited by the fact that the PLA degradation process was not evaluated in vivo. The PLA fiber component is expected to act as a spacer, by which the metallic core can be properly introduced, positioned, and fixed at the target site, and to be degraded after the metallic core has been fixed. However, once placed in the body, it is not possible to control the reaction speed of PLA hydrolyzation. Loco-regional conditions at the target site, such as the existence of bacteria, influence the hydrolyzation reaction, which may result in insufficient fixation of the metallic core due to unexpectedly early PLA degradation, or in disturbance in stent removal due to persistence of unhydrolyzated PLA fibers. Thus, further experimental studies in vivo are warranted.

Another limitation is the choice of material for the metallic component of the hybrid stent. As ANSI 304-grade stainless-steel wire exhibits irreversible deformity when excessive load is added, deformity of the hybrid stent at 50% diameter reduction may be caused by the physical property of this material. Change in configuration of the hybrid stent under highly compressed conditions should be studied with various combinations of materials.

In conclusion, a hybrid stent comprising a metallic wire and a PLA fiber can preserve effective mechanical strength comparable with an identical PLA-only stent. In addition, it has high retrievability after PLA fiber degradation.

Declaration of interest: The authors report no conflicts of interest. The authors alone are responsible for the content and writing of the paper.

References

1. Lee KW, Im JG, Han JK, Kim TK, Park JH, Yeon KM. Tuberculous stenosis of the left main bronchus: results of treatment with balloons and metallic stents. J Vasc Interv Radiol 1999;10:352–8.
2. Doniec JM, Schniewind B, Kahlke V, Kremer B, Grimm H. Therapy of anastomotic leaks by means of covered self-expanding metallic stents after esophagogastrectomy. Endoscopy 2003;35:652–8.
3. Filler RM, Forte V, Fraga JC, Matute J. The use of expandable metallic airway stents for tracheobronchial obstruction. J Pediatr Surg 1995;30:1050–6.
4. Antón-Pacheco JL, Cabezalí D, Tejedor R, López M, Luna C, Comas JV, et al. The role of airway stenting in pediatric tracheobronchial obstruction. Eur J Cardiothorac Surg 2008;33:1069–75.
5. Noppen M, Stratakos G, D'Haese J, Meysman M, Vinken W. Removal of covered self-expandable metallic airway stents in benign disorders: indications, technique, and outcomes. Chest 2005;127:482–7.
6. Matsushita M, Takakuwa H, Nishio A, Kido M, Shimeno N. Open-biopsy-forceps technique for endoscopic removal of distally migrated and impacted biliary metallic stents. Gastrointest Endosc 2003;58:924–7.
7. Tunçözgür B, Savaş MC, Işik AF, Sarimehmetoğlu A, Sanli M, Elbeyli L. Removal of metallic stent by using polyflex stent in esophago-colic anastomotic stricture. Ann Thorac Surg 2006;82:1913–4.
8. Song HY, Shim TS, Kang SG, Jung GS, Lee DY, Kim TH, et al. Tracheobronchial strictures: treatment with a polyurethane-covered retrievable expandable nitinol stent-initial experience. Radiology 1999;213:905–12.
9. Miura S, Yoshioka T, Furuichi K, Tanaka T, Kichikawa K, Ohishi H. Mechanical strength of biliary metllic stents: an experimental comparison. Nippon Acta Radiol 2003;63:201–9.
10. Freitag L, Eicker R, Linz B, Greschuchna D. Theoretical and experimental basis for the development of a dynamic airway stent. Eur Respir J 1994;7:2038–45.

Neurol Med Chir (Tokyo) 49, 179～183, 2009

Percutaneous Vertebroplasty Under Three-Dimensional Radiography Guidance

—Technical Note—

Hiroshi TENJIN, Ayako MANDAI, Daisuke UMEBAYASHI, Shinji YAMAMOTO, Yasuhiko OSAKA, Yoshikazu NAKAHARA, and Noboru TANIGAWA*

Department of Neurosurgery, Kyoto Second Red Cross Hospital, Kyoto;
**Department of Radiology, Kansai Medical University Hirakata Hospital, Hirakata, Osaka*

Abstract

An accurate, safe, and convenient method for performing percutaneous vertebroplasty (PVP) under three-dimensional (3D) radiography guidance has been developed. Six PVP procedures were performed in 5 elderly stroke patients complaining of back pain caused by compressive fracture which interfered with further rehabilitation. T_1-weighted magnetic resonance imaging showed low intensity and T_2-weighted imaging showed high intensity in the fractured vertebral body. The most suitable trajectory for passing the lateral mass of the lamina and pedicle, and reaching the vertebral body was identified on the axial view of 3D radiography. A 13-gauge needle was advanced appropriately in all patients, and improvement of back pain was obtained after injection of polymethylmethacrylate. No major complications occurred in any patient. PVP under 3D radiography guidance is an accurate, safe, and convenient method.

Key words: percutaneous vertebroplasty, three-dimensional radiography, vertebral compression fracture

Introduction

The incidence of osteoporotic vertebral compression fracture is increasing and has become a socioeconomic problem. Back pain resulting from compressive vertebral fracture severely diminishes the activities in daily living (ADL) of the elderly. Compressive vertebral fracture is usually treated conservatively to avoid general anesthesia in an elderly patient. However, conservative therapy requires strict bedrest or the wearing of a hard corset for quite a long time, so may induce further complications. Recently, percutaneous vertebroplasty (PVP) using polymethylmethacrylate (PMMA) has become established for the treatment of painful, osteoporotic compressive vertebral fracture,[3,11] which corrects the pseudoarthrosis,[5,13] and thus obtains early pain relief. PVP is an effective treatment for patients with compressive vertebral fracture allowing early rehabilitation. More accurate, safe, and convenient techniques for PVP would be useful for patients with painful vertebral compressive fracture, because such patients are usually quite old and any complications would severely limit their ADL.

Here we describe a technique for performing PVP under three-dimensional (3D) radiography guidance.

Received May 14, 2008; Accepted December 26, 2008

Treatment Technique

Six PVP procedures were performed in 5 female patients aged from 80 to 85 years using 3D radiography guidance. These patients had suffered stroke before admission, and had developed osteoporotic compressive vertebral body fracture (Table 1). Thus, all patients required early rehabilitation to avoid becoming bedridden. All patients complained of back pain at the level of the compressive fracture, and the fracture interfered with further rehabilitation. Four PVPs were performed for compressive fractures of lumbar vertebrae and two for compressive fractures of thoracic vertebrae (T9 and T11). Compression fracture was mild or moderate, as indicated by loss of more than 30% of the original vertebral height.[2] T_1-weighted magnetic resonance (MR) imaging showed low intensity and T_2-weighted

Table 1 Summary of cases

Case No	Age (yrs), Sex	Complication disease	Fracture level	Delay from onset of fracture to PVP	Delay from onset of complication disease to PVP	Consciousness before PVP (Japan Coma Scale)	Activity of daily living	
							Before PVP	After PVP
1	85, F	hypertensive cerebellar hemorrhage	L2	1 mo	3 wks	I-3	she could not roll over due to back pain	she was able to sit
2	80, F	hypertensive intracerebral hemorrhage	L1	5 yrs	1 mo	I-2	she could not sit for 5 min due to back pain	she was able to sit for 30 min
3	80, F	multiple cerebral infarction	L1	7 days (fall in the ward)	1 yr	I-2	she could not stand up due to back pain	she was able to walk with help
4	83, F	intraventricular hemorrhage	L1	3 mos	2 wks	I-1	she was bed ridden due to back pain	she was able to stand up
5	80, F	cerebral infarction	T9, T11	10 yrs	1 mo	I-1	she could not roll over due to back pain	she did not complain of back pain

PVP: percutaneous vertebroplasty.

MR imaging showed high intensity in the fractured vertebral body,[1,5,12,14] which indicate probable chronic development of pseudoarthrosis in the compressive fracture.[5,13] Written informed consent was obtained from each patient prior to the procedure. There was no financial relationship between the investigators and the study subjects.

Transpedicular PVP was performed under local anesthesia in the angiography room under 3D radiography guidance (Allura Xper FD20; Royal Philips Electronics, Best, The Netherlands). The patients were placed in the prone position on the fluoroscopy table. A marker (FAST FIND GRID; E-Z-EM, Inc., West Bury, N.Y., U.S.A.) was attached to the back and the first rotation scan was obtained. The appropriate window level and width were chosen to include both the vertebral bone and the metal marker. The axial view that included the lamina, pedicle, and body of the vertebra was composed using a 3D workstation (Integris 3D-RA; Royal Philips Electronics) (Fig. 1). The most suitable point for needle insertion was determined, with the trajectory passing the lateral mass of the lamina and pedicle, and reaching the anterior one-third of the vertebral body close to the midline on the axial view using a pilot needle during the second rotation scan (Fig. 2).

The tip of a 13-gauge needle (Osteo-Site Bone Biopsy Needle Murphy M2, length 10 cm; Cook, Bloomington, Ind., U.S.A.) was inserted into the cortex at the lateral mass of the lamina and the third rotation scan was obtained. The trajectory was confirmed on both the axial view and the lateral view (Fig. 3). Then, the needle was advanced under lateral fluoroscopic guidance to reach the anterior one-third of the vertebral body close to the midline,

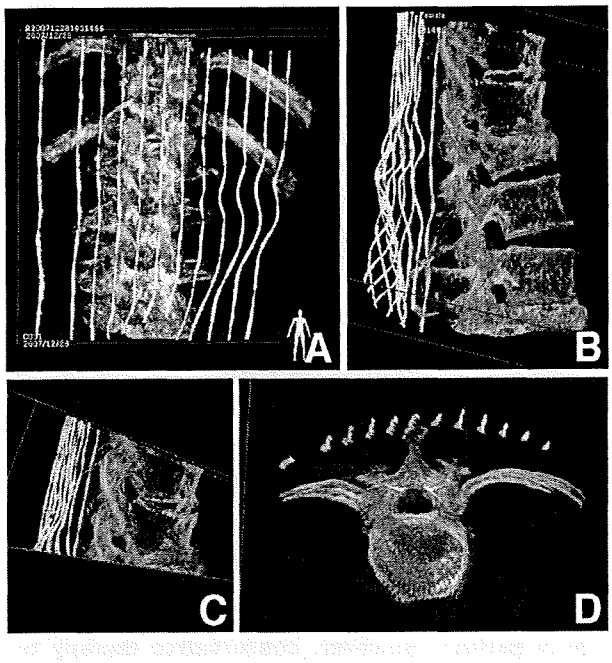

Fig. 1 Three-dimensional radiographs after attaching a marker to the back of the patient. A: Anteroposterior view; B: lateral view; C: lateral view, including the plane passing through the lamina, pedicle, and body of the vertebrae; D: axial view.

when a fourth rotation scan was obtained to confirm the position of the needle tip (Fig. 4). Intraosseous venography was performed with 2–3 ml iopamidol (iodine concentration 300 mg/ml) to confirm that the needle was not within a direct venous anastomosis to the central or epidural veins. Then, 20 g of

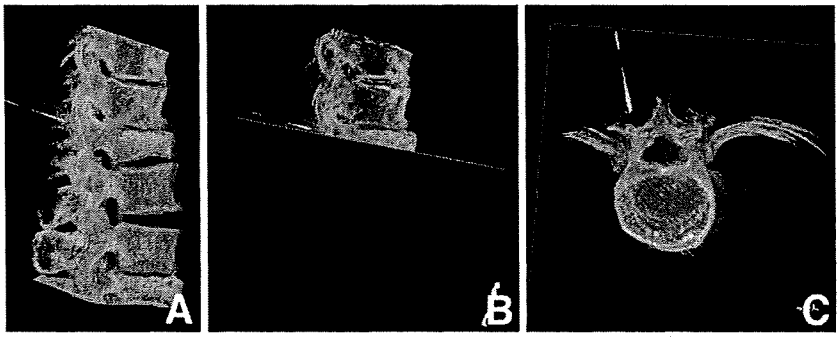

Fig. 2 Three-dimensional radiographs after insertion of the pilot needle. A: Lateral view; B: lateral view, including the plane parallel to the pilot needle; C: axial view.

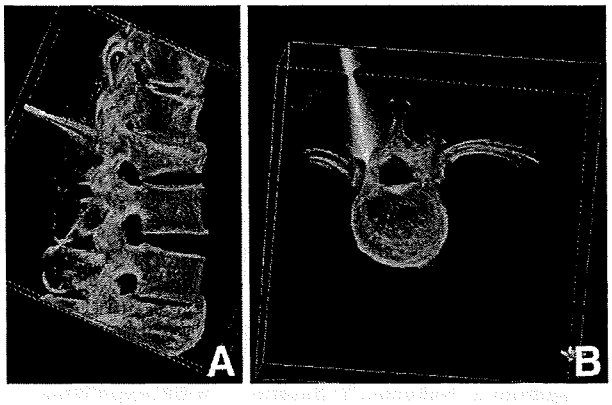

Fig. 3 Three-dimensional radiographs with the tip of a 13-gauge needle inserted into the cortex at the lateral mass of the lamina. A: Lateral view, B: axial view.

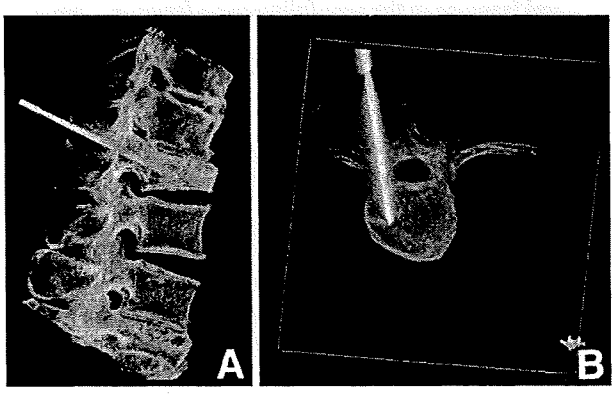

Fig. 4 Three-dimensional radiographs after the tip of a 13-gauge needle had reached the anterior one-third of the vertebral body. A: Lateral view, B: axial view.

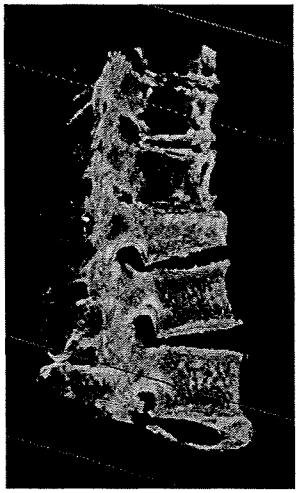

Fig. 5 Three-dimensional radiograph after injection of polymethylmethacrylate (lateral view).

PMMA-styrene powder (Osteobond copolymer bone cement; Zimmer, Warsaw, Ind., U.S.A.) was mixed with 5 g of barium sulfate powder sterilized with dry heat to increase the opacity. Ten ml of liquid methylmethacrylate monomer (Osteobond copolymer bone cement) was added to the powder to produce PMMA. Using 1 ml syringes, the PMMA was injected under lateral fluoroscopic guidance. PMMA injection was terminated when adequate filling of the vertebral body was achieved with 2-3 ml of PMMA. A fifth rotation scan was performed to assess the result (Fig. 5).

The 13-gauge needle was advanced appropriately in all patients. There were no complications except for harmless cement leakage into the disk space in one patient. After the procedure, all patients were observed in the supine position for 1 day. The

patients were followed up by physical examinations and radiography at 1, 3, and 7 days, 3 months, and 1 year after the procedure. The level of ADL just before PVP was compared with that 2 days after PVP to assess improvement. Improvement of back pain was obtained in all patients after PVP (Table 1).

Discussion

PVP is usually performed under guidance using single plane or biplane fluoroscopy,[6,9] or a combination of computed tomography (CT) and fluoroscopy.[4,14] The present study shows that the needle tip can be advanced through the pedicle and into the pseudoarthrosis under 3D radiography guidance, which is more accurate, safe, and convenient compared with previously described methods. Single plane or biplane fluoroscopy cannot provide information regarding the Z axis in real time. Therefore, the appropriate trajectory cannot be determined if deformity of the vertebra is severe. CT and fluoroscopy guidance requires movement of a portable fluoroscopy unit in the CT room, except in the few institutes that have a special room that already contains both CT and fluoroscopy equipment. The image intensifier of portable fluoroscopy equipment is small and low performance, so the resolution on the lateral view is not good even if the CT resolution is better than 3D radiography. Furthermore, the operation area is quite narrow and movement of the fluoroscopy equipment is not convenient. Radiation exposure during PVP is around 130 mGy for 3D radiography (rotation scan 20 mGy/mal × 5 + fluoroscopy 15 mGy/min × 2 min), compared to around 120 mGy for biplane fluoroscopy (30 mGy/min × 4 min), and 330 mGy for CT and fluoroscopy (CT 60 mGy/mal × 5 + fluoroscopy 15 mGy/min × 2 min).

PVP under 3D radiography guidance provides several advantages over conventional methods, and the radiation exposure is comparable or less. We could perform PVP in stroke patients with compressive vertebral fracture to allow early rehabilitation. However, the long-term effects of PVP remain controversial.[7,8,10,15] Several studies have reported new compression fractures in adjacent vertebrae after PVP.

References

1) Baker LL, Goodman SB, Perkash I, Lane B, Enzmann DR: Benign versus pathologic compression fractures of vertebral bodies: Assessment with conventional spin-echo, chemical-shift, and STIR MR imaging. *Radiology* 174: 495–502, 1990
2) Cotton A, Boutry N, Cortet B, Assaker R, Demondion X, Leblond D, Cbastanet P, Duquesnoy B, Dermond H: Percutaneous vertebroplasty: State of art. *Radiographics* 18: 311–323, 1998
3) Deramond H, Depriester C, Galibert P, Le Gars D: Percutaneous vertebroplasty with polymethylmethacrylate. Technique, indications, and results. *Radiol Clin North Am* 36: 533–546, 1998
4) Gangi A, Kastler BA, Dietermann JL: Percutaneous vertebroplasty guided by a combination of CT and fluoroscopy. *AJNR Am J Neuroradiol* 15: 83–86, 1994
5) Hasegawa K, Homma T, Uchiyama S, Takahashi H: Vertebral pseudarthrosis in the osteoporotic spine. *Spine* 22: 2201–2206, 1998
6) Jensen ME, Evans AJ, Mathis JM, Kallmes DF, Cloft HJ, Dion JE: Percutaneous polymethylmethacrylate vertebroplasty in the treatment of osteoporotic vertebral body compression fractures: Technical aspects. *AJNR Am J Neuroradiol* 18: 1897–1904, 1997
7) Kim SH, Kang HS, Choi JA, Ahn JM: Risk factors of new compression fractures in adjacent vertebrae after percutaneous vertebroplasty. *Acta Radiol* 45: 440–445, 2004
8) Komemushi A, Tanigawa N, Kariya S, Kojima H, Shomura Y, Komemushi S, Sawada S: Percutaneous vertebroplasty for osteoporotic compression fracture: Multivariate study of predictors of new vertebral body fracture. *Cardiovasc Intervent Radiol* 29: 580–585, 2005
9) Koyama M, Takizawa K, Kobayashi K, Sasaka K, Hoshikawa Y, Nakaji S, Okamoto K, Kanai N, Okamoto E, Nakajima Y, Sasano Y: Initial experience of percutaneous vertebroplasty using single-plane C-arm fluoroscopy for guidance. *Radiat Med* 23: 256–260, 2005
10) Lindsay R, Silverman SL, Cooper C, Hanley DA, Barton I, Broy SB, Licata A, Benhamou L, Geusens P, Flowers K, Stracke H, Seeman F: Risk of new vertebral fracture in the year following a fracture. *JAMA* 285: 320–323, 2001
11) McGraw JK, Cardella J, Barr JD, Mathis JM, Sanchez O, Schwartzberg MS, Swan TL, Sacks D: Society of interventional radiology quality improvement guidelines for percutaneous vertebroplasty. *J Vasc Interv Radiol* 14: 827–831, 2003
12) Stallmeyer MJB, Zoarski GH, Obuchowski AM: Optimizing patient selection in percutaneous vertebroplasty. *J Vasc Interv Radiol* 14: 683–696, 2003
13) Taneichi H, Kaneda K, Oguma T, Kokaji M: [Risk factor analysis for osteoporotic vertebral collapse and pseudoarthrosis]. *Rinsho Seikei Geka* 37: 437–442, 2002 (Jpn)
14) Tanigawa N, Komemushi A, Kariya S, Kojima H, Shomura Y, Ikeda K, Omura N, Murakami T, Sawada S: Percutaneous vertebroplasty: Relationship between vertebral body bone marrow edema pattern on MR images and initial clinical response. *Radiology* 239: 195–200, 2006
15) Tanigawa N, Komemushi A, Kariya S, Kojima H,

Shomura Y, Sawada S: Radiological follow-up of new compression fractures following percutaneous vertebroplasty. *Cardiovasc Intervent Radiol* 29: 92–96, 2006

Address reprint requests to: Hiroshi Tenjin, M.D., Department of Neurosurgery, Kyoto Second Red Cross Hospital, Kamanza Maruta-machi, Kamigyo-ku, Kyoto 602–8026, Japan.
e-mail: htenjin@nn.iij4u.or.jp

Commentary

I agree with the authors that the incidence of osteoporotic vertebral compressions will become greater in the next future, particularly due to an increase of the expectancy of life. Therefore, the minimally invasive treatment of these fractures in the elderly will become an everyday necessity. The simpler and safer is the procedure, the more the patients will benefit from it, and in a larger number. All these reasons make this paper by H. Tenjin et al. an useful contribution to the problem. The three-dimensional radiography guidance allows even a non-expert to approach correctly the vertebral body percutaneously through the peduncle, in a safe and effective way. I think that, when research provides better bio-materials, possibly the same procedure will be applied to young patients as well, and not just to elderly ones, as the authors have correctly done in this work.

Alessandro DUCATI, *M.D.*
Ordinario di Neurochirurgia
Universita' di Torino
Torino, Italy

4. 集学的治療
c) 集学的治療における肝動注化学療法の位置づけ*

山浦秀和　稲葉吉隆
佐藤洋造　加藤弥菜　金本高明**

〔要旨〕肝転移には肝動注を行う．この治療を当然のように考え行っていたが，全身化学療法の発達に伴い，その位置づけは大きく変化してきた．今回，われわれの施設で行われている肝動注化学療法の現状から「集学的治療における肝動注化学療法の位置づけ」について説明するとともに，肝動注化学療法を行うにあたって，最低限必要な留置法・管理法についても説明する．

はじめに

当院は愛知県という地域柄，患者には中日ドラゴンズのファンが多く，筆者が横浜ベイスターズを応援していることを伝えると，大抵なぐさめの言葉が返ってくる．それはそれとして，最近の野球は先発，中継ぎ，抑えとピッチャーの役割分担がきっちりしていて，その采配は大きく試合結果に影響してくる．肝転移に対する治療戦略も同様で，手術，全身化学療法，肝動注化学療法（以下，肝動注）を目的に合わせて投入する采配が重要なのである．本文の内容は筆者の個人的な所見になるかもしれないが，肝動注を行ううえでの一参考にしていただけたらと思う．

キーワード：肝動注化学療法，集学的治療

* Hepatic arterial infusion chemotherapy in multidisciplinary treatment of liver metastases from colorectal cancer

** H. Yamaura（医長），Y. Inaba（部長），Y. Sato（医長），M. Kato（医長），T. Kanamoto（医長）：愛知県がんセンター中央病院放射線診断・IVR部（〒464-8681　名古屋市千種区鹿子殿1-1）．

1. 肝動注リザーバー留置と管理

肝動注を効果的なものとするには，カテーテル留置はもとより，その後の肝動注の管理こそが重要である．方法論については，今年で34回を迎えるリザーバー研究会で長年にわたって検討され，ほぼ完成したものとなっている．しかし，それらはあまり普及することなく，肝動注という漠然とした治療法だけが普及してしまっていることが，肝動注が誤った評価を受ける要因となっている．よって，まず最低限必要な肝動注リザーバーの留置法・管理法について，リザーバー研究会では常識となっている基本事項を説明したい．なんでも基礎が大切なのである．

1. カテーテル留置の常識―血流改変と胃十二指腸動脈（GDA）-coil法

われわれは放射線科医でありながら大腸癌の全身化学療法にも携わっており，他院からの紹介患者を引き受けることもある．なかには，すでに肝動注リザーバーが留置されているケースもあるが，残念ながらカテーテルが留置されたX線写真の前で感心させられることはほとんどない．5Frのカテーテルが総肝動脈に突き刺すように投げ込まれていることがいまだに経験される．

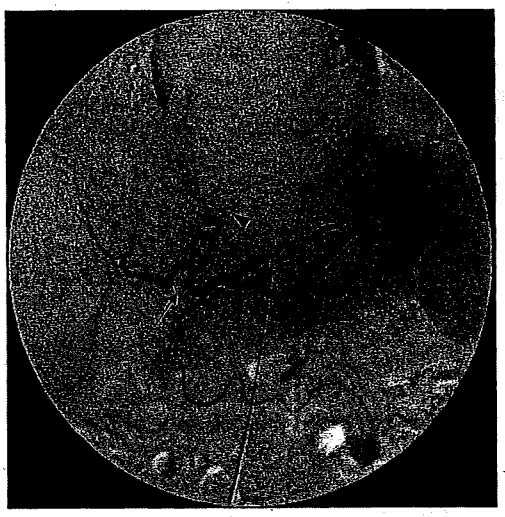

a. DSA. 右胃動脈(矢印)と副左胃動脈(矢頭)をカテーテル留置の前に塞栓する必要がある.

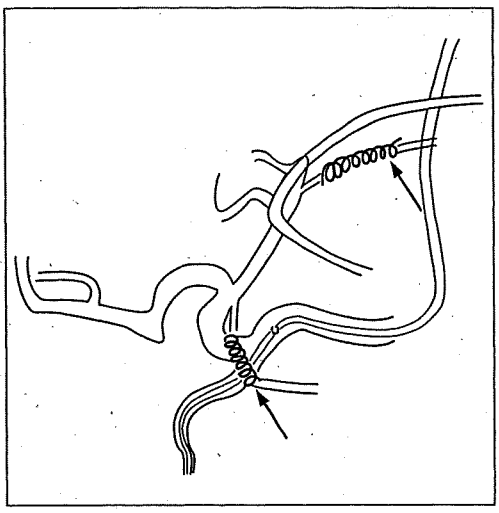

b. シェーマ(1). 副左胃動脈と右胃動脈をマイクロコイルで塞栓後, 留置カテーテルに側孔をあけて, 胃十二指腸動脈へと挿入する.

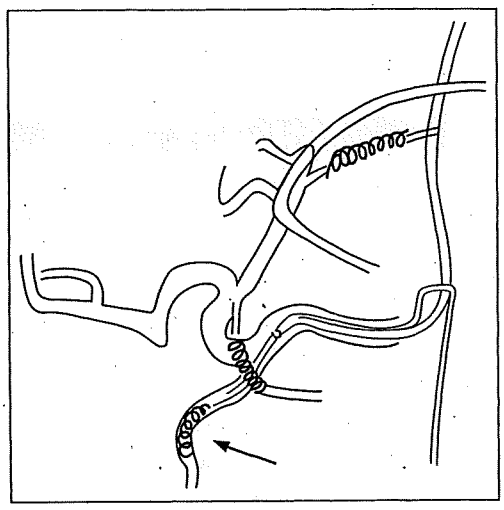

c. シェーマ(2). 別ルートで挿入したマイクロカテーテルを用いて, カテーテルごと胃十二指腸動脈のコイル塞栓を行う(矢印).

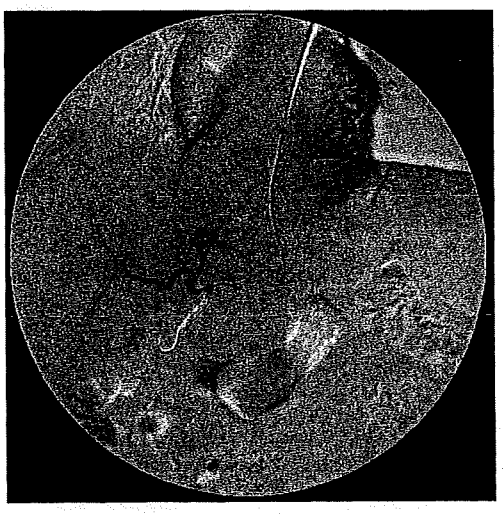

d. 留置カテーテルからのDSA

図1. GDA-coil法によるカテーテル留置. 大腸癌肝転移例

肝動注において最低限必要とされることは, 全肝に薬剤を分布させること, そして肝外へは薬剤を流さないことである. カテーテルを留置する前にきちんと解剖を把握し, 複数本の肝動脈が存在する場合はコイル塞栓による一本化を行う. 一般的にGDAが分岐する肝動脈を残して, ほかを塞栓することが推奨される. 肝外への薬剤流出は消化器毒性を引き起こすため, その原因となる血管も塞栓する必要がある. それには右胃動脈(RGA)の塞栓が行われるほか, 副左胃動脈(ALGA)もまれならず塞栓対象として存在するため注意が必要である. 留置カテーテルの挿入ルートは大腿でも, 鎖骨下動脈でもどちらでもよいが, 従来行われていた総肝動脈への投げ込みは, カテーテル移動の頻度が高く, またカテーテル先端部での機械的刺激により肝動脈閉塞が生じ

るという理由で，現在行うことはまずない．1996年に竹内ら[1]により側孔型カテーテルを用いたGDA-coil法が報告されて以来，これが標準的な留置法とされており，GDAが結紮でもされていない限りこの留置法を行うことが常識である（図1）．

2．動注管理の常識——フローチェックとフローコントロール

肝動注を継続していると肝動脈は徐々に狭小し，やがて途絶してしまう．GDA-coil法における肝動脈の累積開存率は6ヵ月で91.0％，1年で81.4％と報告されており[2]，肝動脈が閉塞していることを知らずに肝動注を行うと，腹痛や胃潰瘍などの合併症を引き起こすことになりかねない．では，肝動脈の開存のみ透視で確認すればよいかというと，そうではない．フローチェックは，透視像に加えてリザーバーからのCT，またはMRIで肝内分布を確認することが必要である．特に尾状葉や後区域に位置する腫瘍は容易に肝外血流を引き込み，それが効果不良の原因となることは常識である．その際，右下横隔動脈が寄生栄養として関与していることが多く，N-butyl-cyanoacrylate（NBCA）〔ヒストアクリル：ビー・ブラウン社〕を用いた鋳型状塞栓を行うことで解決する（図2）．ヒストアクリルが使えない場合は，iodized oil（Lipiodol）/mitomycin（MMC）/gelatin砕片混合物を用いた方法も紹介されているので参考にするとよい[3]．

3．患者管理の常識——動注による副作用

「肝動注は副作用が強いし，トラブルも多い」．以前，他科の先生と話をしていて耳にした言葉である．肝動注技術の水準を疑わざるをえない．肝動注は副作用が少なく，カテーテルを留置して退院すれば1年以上，入院を必要としないこともざらである．多少の食欲低下を訴えることはあるが，全身化学療法を経験した患者からは，その副作用の少なさに必ずといっていいほど感謝される．では，まれな副作用を訴える場合，特に腹痛を訴えるときは肝動脈に何か起きていることを疑うのが常識である．もちろんよいことではない．たいてい肝動脈閉塞であり，リザーバーdigital subtraction angiography（DSA）を行って確認すると肝動脈が描出されない．

しかし，「肝動脈が描出されない≠肝動脈閉塞」も常識である．留置されたカテーテルは2週もすれば部分的に血管壁に固定され始め，1ヵ月もすれば血管壁に埋もれてくる．時にそのフィブリン膜は薬剤流出のための側孔を塞いでしまい，血管は開存しているのにリザーバーからは肝動脈が描出されないという偽閉塞を生じることがある[4]．

II．集学的治療における肝動注化学療法の位置づけ

いよいよ，本題である．FOLFOX/FOLFIRI〔fluorouracil（5-FU）+ levofolinate（*l*-LV）+ oxaliplatin（L-OHP）/5-FU + *l*-LV + irinotecan（CPT-11）〕が切除不能大腸癌の標準治療と位置づけられた現在，もはや「肝転移があるから肝動注」ではない．しかし，件数こそ減ったものの肝動注を行う機会はまだまだあり，それは，原発巣の術前，高度肝転移例，全身化学療法のつなぎ，全身化学療法後といった状況に合わせた肝動注の起用である．これらがどの程度意義のあるものか不明な点も多いが，われわれは模索しながら行っている．

1．術前治療としての肝動注

肝機能障害を有する同時性肝転移例の場合，原発巣の手術はタイミングを誤ると，術後に急速な肝転移の進行から高度の肝機能障害をきたし，抗癌治療を開始する機会もなく肝不全に陥ることがある．原発巣の手術を行うかどうかは，個々の背景や施設の方針によって異なるが，Iguchiら[5]は肝動注を行うことによって安全に原発巣の切除ができることを報告している．この役割は全身化学療法でも代用可能であるが，FOLFOXは術前に最低3週間，bevacizumabが加われば6週間の休薬期間が推奨されており，休薬期間中に病変が急速に増大することが危惧される．また，術後も最低2週間は化学療法の再開はできず，術後の経過が思わしくなければ，リスクの高い状態で化学療法を再開することが余儀なくされる．一方肝動注は，全身状態に影響を与えることなく治療を行うことが可能であり，術前後は1週間の休薬で問題ない．

2．高度肝転移例への肝動注

肝転移が高度な場合，それが予後規定因子となる可能性が高く，まず肝転移を抑えることが予後の延長に寄与する可能性がある．ALP 600IU/*l*以上の肝転移を対象とした場合，FOLFOXと肝

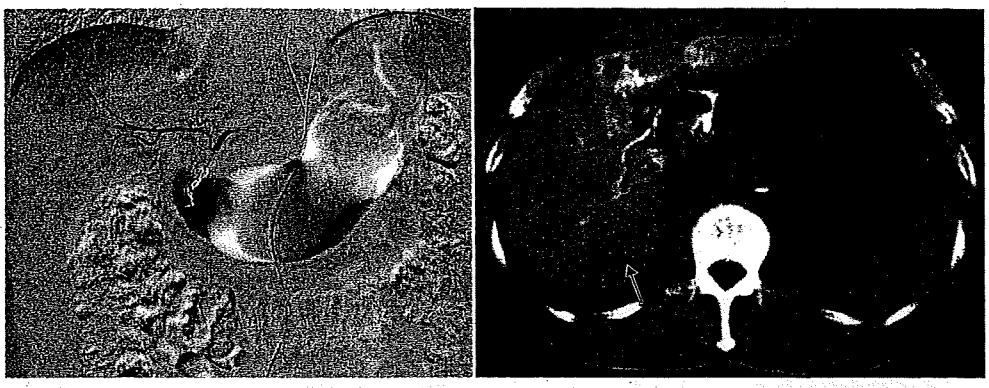

a. リザーバーDSA(左)と留置後3ヵ月リザーバーCT(右). DSAでの異常は認識できないが, リザーバーCTでは後区域腫瘍への分布が認められない(右図:矢印).

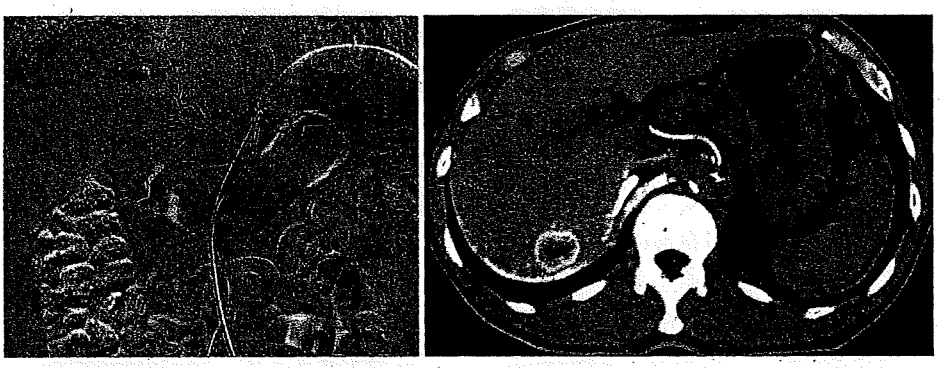

b. 右下横隔動脈のDSA(左)とCTA(右). 右下横隔動脈から後区域腫瘍への寄生栄養を認める.

c. 血流改変術後X線像(左)と2ヵ月後リザーバーCT(右). ヒストアクリルとLipiodolの混合液(6:1)で鋳型上の塞栓(左図:矢印)を行うことで、リザーバーからの分布が改善し腫瘍も縮小した(右図:矢印).

図2. 右下横隔動脈に対する血流改変術

動注の奏効率はそれぞれ40%, 57%と報告されており[6], 全身化学療法よりも肝動注を先行するという戦略も妥当性がある.

しかし, 実際の臨床現場では標準治療という看板と, すぐに開始できる手軽さから肝動注が選ばれることはまずなく, よほどのperformance status不良例しか放射線科へのコンサルトがないのが現状である.

これに関しては, リザーバー研究会と日本インターベンショナルラジオロジー研究グループ(JIVROSG)を中心に, ALP 600IU/*l*以上の肝転移例を対象としたFOLFOX先行群と肝動注先行

Jpn J Clin Oncol 2009;39(6)406–409
doi:10.1093/jjco/hyp035

Clinical Trial Note

A Randomized Phase II/III Trial Comparing Hepatectomy Followed by mFOLFOX6 with Hepatectomy Alone as Treatment for Liver Metastasis from Colorectal Cancer: Japan Clinical Oncology Group Study JCOG0603

Yukihide Kanemitsu[1], Tomoyuki Kato[2], Yasuhiro Shimizu[1], Yoshitaka Inaba[3], Yasuhiro Shimada[4], Kenichi Nakamura[5], Akihiro Sato[6] and Yoshihiro Moriya[7] for the Colorectal Cancer Study Group (CCSG) of Japan Clinical Oncology Group

[1]Department of Gastroenterological Surgery, Aichi Cancer Center Hospital, [2]Department of Surgery, Kamiiida Daiichi General Hospital, [3]Department of Diagnostic and Interventional Radiology, Aichi Cancer Center Hospital, Nagoya, [4]Department of Gastrointestinal Oncology Division, National Cancer Center Hospital, [5]JCOG Data Center, Center for Cancer Control and Information Services, National Cancer Center, Tokyo, [6]Research Center for Innovative Oncology, National Cancer Center Hospital East, Kashiwa, Chiba and [7]Colorectal Surgery Division, National Cancer Center Hospital, Tokyo, Japan

Received October 22, 2008; accepted March 15, 2009; published online April 23, 2009

A randomized controlled trial is being conducted in Japan to compare hepatectomy alone with hepatectomy followed by adjuvant chemotherapy as treatment in patients with curatively resected liver metastases from colorectal cancer to improve survival with intensive chemotherapy. Between 42 and 70 days after liver resection, patients are randomly assigned to either hepatectomy alone or hepatectomy followed by 12 cycles of modified FOLFOX6 (mFOLFOX6) regimen. A total of 300 patients (including 78 patients in Phase II) will be accrued from 38 institutions within 3 years. The primary endpoint is treatment compliance at nine courses of mFOLFOX6 regimen in Phase II and disease-free survival in Phase III. The secondary endpoints are overall survival, incidence of adverse events and patterns of recurrence.

Key words: colorectal cancer – liver metastases – randomized controlled trial – mFOLFOX6

INTRODUCTION

Approximately one-third of patients survive for 5 years following curative resection of hepatic metastases from colorectal cancer (1,2), and the proportion of hepatectomy-related death is as low as 1–2% (3–5). These observations strongly support the view that hepatectomy seems to be the most effective therapy for treating hepatic metastases from colorectal cancer, due to the potential for long-term survival that is not possible with other treatment modalities. However, a hepatectomy alone does not always provide a complete cure. Most recurrences occur in liver, lung or both within the first 2 years after hepatectomy. Adjuvant chemotherapy may reduce the risk of recurrence and improve long-term survival, but administering systemic agents to the patients with resectable hepatic metastases in the clinical practice is not universal. In their EORTC40983 trial, Nordlinger et al. (6) identified a prominent need for a well-conducted randomized trial to compare hepatectomy alone with combined hepatectomy and chemotherapy treatment in patients with resectable colorectal liver metastases. However, we question the strategy to give pre-operative chemotherapy to patients with resectable colorectal liver metastases, as this postponed a possible curative treatment. Patients who receive pre-operative chemotherapy often have a higher risk toward

For reprints and all correspondence: Yukihide Kanemitsu, Department of Gastroenterological Surgery, Aichi Cancer Center, 1-1 Kanokoden, Chikusa-ku, Nagoya 464-8681, Japan. E-mail: ykanemit@aichi-cc.jp

post-operative complications. Theoretically, post-operative chemotherapy should be effective toward microscopic residual disease in the remnant liver or body. Until the report of the AURC 9002 trial by Portier et al. (7), there was no clear evidence from a randomized trial demonstrating that post-operative chemotherapy, either systemic or by hepatic arterial infusion, was more beneficial than hepatectomy alone. In the 10 years needed to complete accrual for this trial, however, the original question became outdated due to the availability of more effective chemotherapy regimens containing potentially more active agents such as oxaliplatin, irinotecan, bevacizumab or cetuximab. It is therefore still unclear whether combined treatment with post-operative chemotherapy is better than hepatectomy alone in patients with resectable liver metastases from colorectal cancer.

The rationale for choosing FOLFOX regimen as the treatment arm in this trial is based on the results of the previous studies for Stage III patients and unresectable Stage IV patients. Oxaliplatin-based therapy is also a standard first-line treatment for advanced or metastatic unresectable colorectal cancer. We chose the modified FOLFOX6 (mFOLFOX6) regimen for the study, since it is the most convenient of the FOLFOX regimens and can be administered on an outpatient basis. In Japan, however, oxaliplatin was approved in April 2005, and we set a Phase II part in this trial to confirm the feasibility of mFOLFOX6 regimen in the Japanese population with resected liver metastases from colorectal cancer.

Accordingly, we have started a Phase II/III randomized controlled trial to evaluate mFOLFOX6 as post-operative chemotherapy for patients with curatively resected liver metastases from colorectal cancer.

The study protocol was designed by the Colorectal Cancer Study Group (CCSG) of the Japan Clinical Oncology Group (JCOG) and was approved by the Protocol Review Committee of JCOG on 15 February 2007. This trial was registered at the UMIN Clinical Trials Registry as UMIN000000653 (http://www.umin.ac.jp/ctr/index.htm) and was activated on 16 April 2007.

STUDY PROTOCOL

Purpose

The aim of this study is to demonstrate the feasibility (Phase II) and the superiority of disease-free survival (Phase III) of systemic intravenous post-operative chemotherapy with mFOLFOX6 compared with hepatectomy alone in patients with curatively resected liver metastases from colorectal cancer.

Study Setting

The study was a multi-institutional prospective randomized Phase II/III trial, where participating institutions include 38 specialized centers as on 4 September 2008.

Resources

The study was supported by Health and Labour Sciences Research Grants for Clinical Cancer Research (h16-032 and h19-024) and Grants-in-Aid for Cancer Research (17S-3, 17S-5, 20S-3 and 20S-6), from the Ministry of Health, Labour and Welfare, Japan.

Endpoints

The primary endpoint in the Phase II part is treatment compliance at nine courses after beginning mFOLFOX6 [bolus and infusion fluorouracil (FU) and leucovorin (LV) with oxaliplatin] in all eligible patients. Treatment compliance at nine courses is defined as the proportion of patients in whom oxaliplatin is administered nine courses or more according to the protocol. The primary endpoint in the Phase III part is disease-free survival which is defined as days from randomization to first evidence of recurrence, secondary cancer or death from any cause, and it was censored at the latest day when the patient was alive without any evidence of recurrence or secondary cancer.

Secondary endpoints are overall survival, incidence of adverse events defined by Common Terminology Criteria for Adverse Events (CTCAE) version 3.0 and patterns of recurrence after liver resection.

Eligibility Criteria

Primary tumors are staged according to the sixth edition of the tumor-nodes-metastasis classification system of the Union Internationale Contre le Cancer (UICC).

Inclusion Criteria

Prior to enrollment in the study, patients must fulfill all of the following criteria: the resected liver specimen consists of histologically proven adenocarcinoma of the colorectum. Potentially curative R0 resection was performed for both primary tumor and liver metastasis. In metachronous cases, the liver metastasis should be the first and the only recurrence. No extrahepatic metastasis or recurrence on chest and abdominal CT or MRI within 4 weeks before enrollment. No prior chemotherapy with oxaliplatin. No other chemotherapy or radiotherapy within 3 months before enrollment. No prior radiofrequency ablation or cryotherapy for liver metastasis. Time since their hepatectomy is between 42 and 70 days. Age is between 20 and 75 years old. European Cooperative Oncology Group (ECOG) performance status is 0–1. There are sufficient organ functions. Completed written informed consent from patient is obtained.

Exclusion Criteria

Patients are excluded if they meet any of the following criteria: (i) synchronous or metachronous multiple cancer,